

Laser-pulse-shape control of photofragmentation in the weak-field limit

Ashwani K. Tiwari and Diptesh Dey

Indian Institute of Science Education and Research Kolkata, Mohanpur 741 252, India

Niels E. Henriksen*

Department of Chemistry, Building 207, Technical University of Denmark, DK-2800 Kgs. Lyngby, Denmark

(Received 18 October 2013; revised manuscript received 6 December 2013; published 14 February 2014)

We demonstrate theoretically that laser-induced coherent quantum interference control of asymptotic states of dissociating molecules is possible even in the (one-photon) weak-field limit starting from a single vibrational eigenstate. Thus, phase dependence in the interaction with a fixed energy phase-modulated pulse can persist for some time after the pulse is over. This is illustrated for the nonadiabatic process: $I + Br^* \leftarrow IBr \rightarrow I + Br$, where the relative yield of excited Br^* can be changed by pure phase modulation. It is shown that the phase is able to influence wave-packet spreading in the continuum as well as the average internuclear distance in each channel.

DOI: [10.1103/PhysRevA.89.023417](https://doi.org/10.1103/PhysRevA.89.023417)

PACS number(s): 32.80.Qk, 82.20.-w, 82.50.Nd, 82.53.-k

I. INTRODUCTION

The idea that optimized laser fields can guide the dynamics of an atom or molecule from a given initial state into a desired final state has attracted much attention in recent years [1–8]. Consider a molecule ABC which is bound in its electronic ground state and where fragmentation can take place in excited electronic states. A generic problem in laser control concerns the control of a reaction of the type $A + BC \leftarrow ABC \rightarrow AB + C$, in particular, to what extent can one take advantage of the phase coherence of laser pulses in order to change the branching ratio between the two channels $A + BC$ and $AB + C$ as well as the final state distribution within each of these rearrangement channels.

The time-dependent phase-coherent electric field of a laser pulse can be represented by

$$\mathcal{E}(t) = \mathcal{E}_0 \text{Re} \left[\int_{-\infty}^{\infty} A(\omega) e^{i\phi(\omega)} e^{-i\omega t} d\omega \right], \quad (1)$$

where $A(\omega)$ is the real-valued distribution of frequencies and $\phi(\omega)$ is the real-valued frequency-dependent phase. The temporal duration and shape of the pulse depends on the phases whereas the energy in the field $\propto \int |\mathcal{E}(t)|^2 dt \propto \int |A(\omega) e^{i\phi(\omega)}|^2 d\omega = \int |A(\omega)|^2 d\omega$ is independent of the phases. Disregarding effects of varying the frequency distribution of the pulse, pulse shaping is obtained by employing a phase-modulated excitation pulse. Phase modulation in turn will change the magnitude of quantum mechanical interference terms in the interaction with matter; this is the essence of coherent control.

Coherent control in the weak-field (one-photon) limit—where amplitude exclusively is transferred from the electronic ground state to an excited state surface—uses the laser’s phase coherence and exploit quantum (multiple-path) interference in its purest form [2,9] and is a real extension of traditional (incoherent) photochemistry. However, when excitation out of a single eigenstate of ABC is considered and direct

fragmentation takes place within a dissociative continuum of states, a seminal proof showed that no phase control of final state distributions of the fragments [10,11] is possible in the long-time limit.

Laser phase dependence can, however, be observed when weak-field excitation out of a nonstationary superposition of bound vibrational states of ABC is considered. The branching ratio depends, e.g., on the time shift/delay of the laser pulse [12–14], which is related to the linear part of the phase function $\phi(\omega)$.

Beyond the weak-field limit, coherent control plays an important role in the pulsed strong-field excitation out of a single stationary vibrational state of ABC. In the strong-field limit, amplitude can be transferred from the electronic ground state to an excited electronic state and back to the electronic ground state. This can lead to a nonstationary superposition of bound vibrational states of ABC which subsequently is transferred to an excited electronic state where fragmentation takes place [15,16]. The optimal pulse shape can often be decomposed into properly timed pump and dump pulses between various potential energy surfaces. These pulses are based on proper time delays and pulse shapes, i.e., coherent control plays again an important role. The use of strong fields create, however, potential problems with the population of unwanted channels, e.g., related to ionization.

Recently, the weak-field excitation out of a single stationary state has attracted considerable renewed attention [17–23]. Thus, a reinvestigation of the circumstances under which weak-field coherent control is possible has been undertaken. As mentioned above, for direct fragmentation in the long-time limit, it has been shown that such control is not possible [10].

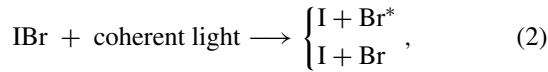
Phase dependence of isomerization yields has been reported recently in the weak-field limit [17–20]. It was shown that phase dependence can persist over long times when the few modes that are active in the isomerization are coupled intramolecularly to the many vibrational modes in a large molecule or, in general, to an external environment. This coupling allows for dissipation of energy from the isomerization coordinates and effectively constrains the observables to finite times of the system dynamics.

*neh@kemi.dtu.dk

We show here that a phase dependence associated with a fixed bandwidth phase modulated pulse can be observed and persists for some time after the pulse is over—also for direct fragmentation within an isolated dissociative continuum with a few degrees of freedom. Not only the total dissociation probability [22,23] but also the branching ratio between two channels can be modified. It is shown that the phase is able to influence wave-packet spreading in coupled continua and, remarkably, also the average position in each channel.

II. MOLECULAR SYSTEM AND THEORETICAL/COMPUTATIONAL APPROACH

We consider in the following the fragmentation of a diatomic molecule leading to atomic fragments in two different electronic states. Specifically, we consider the process,



where Br^* is the spin-orbit excited $\text{Br}(^2\text{P}_{1/2})$. The relevant potential energy curves for IBr [24–26] are shown in Fig. 1. The two excited state potentials interact with each other around their crossing at an internuclear distance of about 6 a.u., which leads to the ground and excited adiabatic states. We consider in the following laser excitation out of the vibrational and electronic ground state at a center wavelength of $\lambda_0 = 530$ nm. Essentially direct dissociation takes place for $\lambda < 545$ nm, which is above the dissociation limit for both channels. This three-state model [25] works well at low energies (i.e., $\lambda > 500$ nm) additional excited electronic states are involved at higher energies [24].

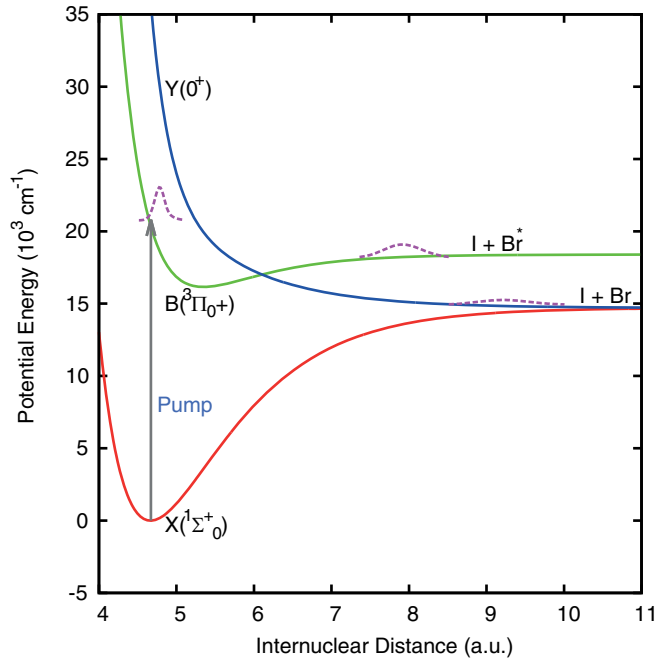


FIG. 1. (Color online) The relevant potential energy curves of IBr and sketch of the wave packet after vertical excitation. Due to the nonadiabatic crossing, the wave packet bifurcates into the two channels $\text{I} + \text{Br}^*$ and $\text{I} + \text{Br}$. At a fixed time, the wave packets have different average distances and associated spreadings.

For simplicity, we consider an electric field corresponding to a Gaussian frequency distribution (centered at ω_0) with a quadratic phase function [27], i.e.,

$$A(\omega)e^{i\phi(\omega)} = \sqrt{\frac{\tau_0^2}{2\pi}} e^{[-\tau_0^2(\omega-\omega_0)^2/2 + i\beta_0(\omega-\omega_0)^2/2]}, \quad (3)$$

where $1/\tau_0$ is the frequency bandwidth and β_0 is the linear spectral chirp. The time-dependent electric field in Eq. (1) then takes the form,

$$\mathcal{E}(t) = \mathcal{E}_0 \text{Re} \left[\sqrt{\frac{\tau_0^2}{\tau_0^2 - i\beta_0}} \exp \left(-\frac{t^2}{2\tau^2} - i\beta t^2/2 - i\omega_0 t \right) \right], \quad (4)$$

with pulse duration τ and linear temporal chirp β , which are related to τ_0 and β_0 via $\beta = \beta_0/(\tau_0^4 + \beta_0^2)$ and $\tau^2 = \tau_0^2(1 + \beta_0^2/\tau_0^4)$.

The spectral chirp introduces a time-dependent frequency distribution of the field in Eq. (4). In the following calculations, we start with a transform-limited pulse ($\beta_0 = \beta = 0$) of duration $\tau_{\text{FWHM}} = \tau\sqrt{8\ln 2} = 30$ fs, keep the bandwidth $1/\tau_0$ fixed, and change then the linear spectral chirp β_0 . We consider laser pulses for $\beta_0 = 1000$ and -1000 fs². With this chirp, the temporal duration of the Gaussian pulse envelope is still within a few hundred femtoseconds, i.e., $\tau_{\text{FWHM}} = 187$ fs.

We treat IBr as a one-dimensional system (see Ref. [25] for details), assuming that the transition dipole moment for the $X \rightarrow B$ transition is oriented in the direction of the field. In this description, the angular momentum of the overall rotational motion, i.e., the centrifugal energy is neglected in the dynamics of the internuclear motion. This is an excellent approximation, at least, for small values of the angular momentum [22]. The laser-induced dynamics is calculated within the electric-dipole approximation and first-order perturbation theory for the interaction with the field. The wave functions, potentials, and coupling element are represented on an equally spaced grid of 1024 points with $3.70 \leq x \leq 20.50$ a.u. An absorbing potential is added for $x \geq 18.4$ a.u. to avoid unphysical reflections into the inner region. The initial wave function in the vibrational ground state is computed using the Fourier-grid Hamiltonian method [28]. In the diabatic representation, the time propagation of wave functions, $\psi_i(x, t)$ where i refers to channel $\text{I} + \text{Br}^*$ or $\text{I} + \text{Br}$, is accomplished by the split-operator method [29].

The atomic fragments are detected spectroscopically with a short probe pulse. The relevant Franck-Condon window function can be approximated by a step function at $x = x_d$, which implies that the probe signal can be evaluated as the time-integrated flux at $x = x_d$ [30]. The probability flux is obtained from

$$J_i(t) = \frac{\hbar}{m} \text{Im} \left[\psi_i^*(x, t) \frac{\partial \psi_i(x, t)}{\partial x} \right]_{x=x_d}, \quad (5)$$

where m is the reduced mass of IBr. The time-integrated flux over $[-\infty, t]$ yields the dissociation probability and is proportional to the time-resolved probe signal,

$$P_i(t) = \int_{-\infty}^t J_i(t') dt'. \quad (6)$$

In the following, we choose $x_d = 10$ a.u. which is within ~ 150 cm $^{-1}$ from the asymptotic value of the potentials. Thus, for a short probe pulse tuned to an atomic transition in the fragments, this point is within the energy spread of the pulse. The intensity of the pump pulse is 1.7×10^{10} W/cm 2 (with a constant transition dipole moment of 1 a.u.), such that the calculations are performed in the weak-field regime.

III. RESULTS AND DISCUSSION

We consider the total dissociation probability in the two channels $I + Br^*$ and $I + Br$ and the relative yield of Br^* , defined as $Br^*/(Br^* + Br)$. Figure 2 shows the total dissociation probability and the relative yield of Br^* as a function of time. The results are shown for different linear spectral chirps. The dissociation is completed at around 600 fs with detection starting at $x_d = 10$ a.u. The general findings are insensitive to the precise choice of x_d . Note that the total dissociation probability is less than 5%; in this weak-field regime the excitation probability depends linearly on laser intensity. As

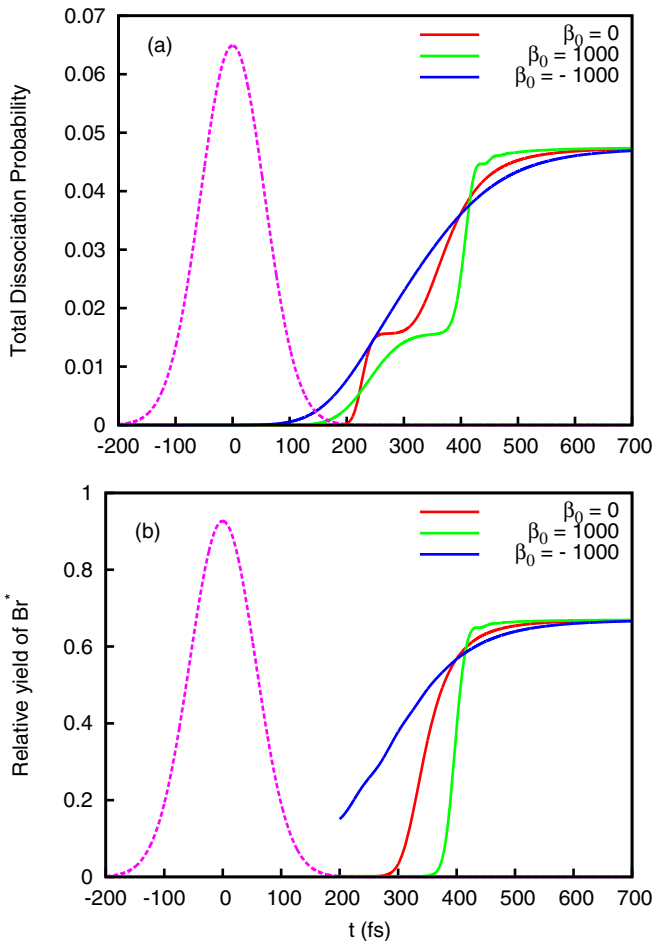


FIG. 2. (Color online) Panel (a) shows the total dissociation probability and panel (b) shows the relative yield of Br^* as a function of time. The results are shown for different linear spectral chirps. The dashed curve to the left shows the pulse envelope of the chirped pulses (in arbitrary unit). The relative yield is plotted after the pulse has decayed and note that all three laser pulses have exactly the same energy.

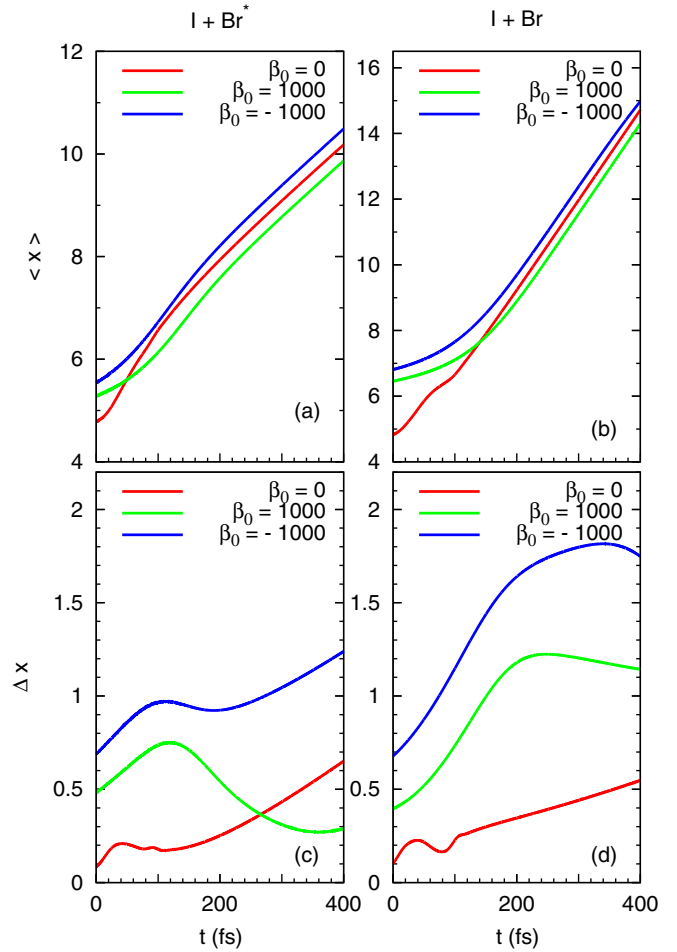


FIG. 3. (Color online) Expectation value of the interatomic distance and the associated spreading (in a.u. of length) for different linear spectral chirps. The results on the left-hand side are for the $I + Br^*$ channel whereas the right-hand side shows the $I + Br$ channel.

expected, the results are independent of chirp in the long-time limit but we observe a clear phase dependence at early times after the pulse has decayed, in particular, in the time interval from 200 to 400 fs.

We checked that the expectation value of the relative momentum (p) as well as the associated uncertainty Δp is independent of chirp—in the long-time limit after 600–700 fs. The $I + Br^*$ channel has the lower relative momentum compared to $I + Br$ due to the higher potential energy.

With the negatively chirped pulse ($\beta_0 = -1000$ fs 2), high momenta are launched first prior to the low momenta. For the positively chirped pulse ($\beta_0 = 1000$ fs 2), low momenta are launched first prior to the high momenta. Comparing Figs. 2(a) and 2(b), we observe that with negative chirp, the total flux in the interval from 200 to 400 fs consists of a mixture of Br and Br^* . For the transform-limited pulse, the flux in the interval from 200–300 fs is pure Br (due to the higher relative speed of Br). With positive chirp, the flux in the interval from 200 to 380 fs is pure Br .

In order to explain the observations in Fig. 2(b), we show in Fig. 3 the expectation values of the interatomic distance $\langle x \rangle$ and the associated uncertainty Δx . It is well known that chirp can change the spreading/focusing of a wave packet and

this phenomenon has previously been analyzed in detail under simple adiabatic dynamics [31–34]. In the present case with nonadiabatic dynamics in coupled continua, we observe that chirp changes Δx and that wave packet focusing can be clearly observed for positive chirp. The spreading/focusing within the first 400 fs is, however, quite different in the two electronic states. It should be noted that all wave packets are outside the crossing region after about 150 fs and, essentially, free after about 200 fs. Figure 3 shows, for all cases, that the expectation value of the interatomic distance $\langle x \rangle$ increases linearly with time at sufficiently long times. This is what one expects for a free wave packet. However, a remarkable effect is observed: The average position of the wave packet can be controlled by the laser chirp! For $I + Br^*$, the smallest values of $\langle x \rangle$ and Δx are obtained for positive chirp, larger values for zero chirp, and the largest values for negative chirp. The implications are, as shown in Fig. 2(b), that Br^* arrives at the “detector” at different times; the appearance of Br^* is delayed going from negative to positive chirp.

IV. CONCLUSIONS

In conclusion, with fragment detection at a given internuclear position, we have shown that phase modulation of a fixed energy laser pulse can modify the branching ratio between two channels in a photofragmentation process. Such phase dependence can persist for some time after the laser pulse has decayed also without any coupling to an external environment. Thus, in a channel-specific way, the laser phase is able to influence wave-packet spreading in the continuum also for nonadiabatic dynamics and, remarkably, also the average position of a wave packet. We considered a direct photofragmentation, however, it is anticipated that even stronger effects could be observed for indirect (resonance) fragmentation [22]. Finally, it is interesting to note that the branching ratio, i.e., the curve-crossing probability in the long-time ($t \rightarrow \infty$) limit, is independent of chirp. The explanation of this observation is clearly outside the scope of the standard Landau-Zener formalism.

-
- [1] S. A. Rice and M. Zhao, *Optical Control of Molecular Dynamics* (Wiley, New York, 2000).
- [2] M. Shapiro and P. Brumer, *Quantum Control of Molecular Processes* (Wiley, New York, 2012).
- [3] C. Brif, R. Chakrabarti, and H. Rabitz, *New J. Phys.* **12**, 075008 (2010).
- [4] A. Assion, T. Baumert, M. Bergt, T. Brixner, B. Kiefer, V. Seyfried, M. Strehle, and G. Gerber, *Science* **282**, 919 (1998).
- [5] T. C. Weinacht, J. Ahn, and P. H. Bucksbaum, *Nature (London)* **397**, 233 (1999).
- [6] R. J. Levis, G. M. Mekir, and H. Rabitz, *Science* **292**, 709 (2001).
- [7] G. Vogt, G. Krampert, P. Niklaus, P. Nuernberger, and G. Gerber, *Phys. Rev. Lett.* **94**, 068305 (2005).
- [8] I. Barth and J. Manz, *Angew. Chem. Int. Ed.* **45**, 2962 (2006).
- [9] P. Brumer and M. Shapiro, *Chem. Phys. Lett.* **126**, 541 (1986).
- [10] P. Brumer and M. Shapiro, *Chem. Phys.* **139**, 221 (1989).
- [11] M. Shapiro and P. Brumer, *J. Phys. Chem. A* **105**, 2897 (2001).
- [12] B. Amstrup and N. E. Henriksen, *J. Chem. Phys.* **97**, 8285 (1992).
- [13] M. Shapiro and P. Brumer, *J. Chem. Phys.* **98**, 201 (1993).
- [14] B. Amstrup and N. E. Henriksen, *J. Chem. Phys.* **105**, 9115 (1996).
- [15] D. J. Tannor and S. A. Rice, *J. Chem. Phys.* **83**, 5013 (1985).
- [16] A. K. Tiwari, K. B. Møller, and N. E. Henriksen, *Phys. Rev. A* **78**, 065402 (2008).
- [17] V. I. Prokhorenko, A. M. Nagy, S. A. Waschuk, L. S. Brown, R. R. Birge, and R. J. Dwayne Miller, *Science* **313**, 1257 (2006).
- [18] V. I. Prokhorenko, A. M. Nagy, L. S. Brown, and R. J. Dwayne Miller, *Chem. Phys.* **341**, 296 (2007).
- [19] G. Katz, M. A. Ratner, and R. Kosloff, *New J. Phys.* **12**, 015003 (2010).
- [20] C. A. Arango and P. Brumer, *J. Chem. Phys.* **138**, 071104 (2013).
- [21] M. Spanner, C. A. Arango, and P. Brumer, *J. Chem. Phys.* **133**, 151101 (2010).
- [22] C. C. Shu and N. E. Henriksen, *J. Chem. Phys.* **134**, 164308 (2011).
- [23] C. C. Shu and N. E. Henriksen, *J. Chem. Phys.* **136**, 044303 (2012).
- [24] E. Wrede, S. Laubach, S. Schulenburg, A. Brown, E. R. Wouters, A. J. Orr-Ewing, and M. N. R. Ashfold, *J. Chem. Phys.* **114**, 2629 (2001).
- [25] H. Guo, *J. Chem. Phys.* **99**, 1685 (1993).
- [26] B. J. Sussman, D. Townsend, M. Yu. Ivanov, and A. Stolow, *Science* **314**, 278 (2006).
- [27] N. E. Henriksen and K. B. Møller, *J. Chem. Phys.* **119**, 2569 (2003).
- [28] C. C. Marston and G. G. Balint-Kurti, *J. Chem. Phys.* **91**, 3571 (1989).
- [29] R. Kosloff, *J. Phys. Chem.* **92**, 2087 (1988).
- [30] N. E. Henriksen and V. Engel, *Int. Rev. Phys. Chem.* **20**, 93 (2001).
- [31] B. Kohler, V. V. Yakovlev, J. Che, J. L. Krause, M. Messina, K. R. Wilson, N. Schwentner, R. M. Whitnell, and Y.-J. Yan, *Phys. Rev. Lett.* **74**, 3360 (1995).
- [32] J. L. Krause, R. M. Whitnell, K. R. Wilson, Y.-J. Yan, and S. Mukamel, *J. Chem. Phys.* **99**, 6562 (1993).
- [33] C. Manescu, J. L. Krause, K. B. Møller, and N. E. Henriksen, *J. Phys. Chem. A* **108**, 8840 (2004).
- [34] A. K. Tiwari, K. B. Møller, and N. E. Henriksen, *Chem. Phys. Lett.* **450**, 6 (2007).